Inorg. Chem. **2005**, *44*, 9464–9470

Synthesis and Characterization of the Open-Framework Barium Bisphosphonate $[Ba_3(O_3PCH_2NH_2CH_2PO_3)_2(H_2O)_4]\cdot 3H_2O$

Sebastian Bauer,[†] Helen Müller,[‡] Thomas Bein,[‡] and Norbert Stock*,[†]

Institute of Inorganic Chemistry, Christian-Albrechts-University, Otto-Hahn-Platz 6/7, 24118 Kiel, Germany, and Department Chemie, Ludwig-Maximilians-Universität München, Butenandtstr. 5-13, Haus E, 81377 München, Germany

Received June 9, 2005

Following the strategy of using polyfunctional phosphonic acids for the synthesis of open-framework metal phosphonates, the phosphonocarboxylic acid $(H_2O_3PCH_2)_2NCH_2C_6H_4COOH$ was used in the hydrothermal synthesis of new Ba phosphonates. Its decomposition led to the first open-framework barium phosphonate $[Ba_3(O_3PCH_2NH_2CH_2PO_3)_2(H_2O)_4]\cdot 3H_2O$ (**1**). The synthesis was also successfully performed using iminobis(methylphosphonic acid), $(H_2O_3PCH_2)_2NH$, as a starting material, and the synthesis was optimized to obtain **1** as a pure material. The reaction setup as well as the pH are the dominant parameters, and only a diffusion-controlled reaction led to the desired compound, **1**. The crystal structure was solved from single-crystal data: monoclinic; *C*2/*c*; $a = 2328.7(2)$, $b = 1359.95(7)$, and $c = 718.62(6)$ pm; $\beta = 98.732(10)°$; $V = 2249.5(3) \times 10^6$ pm^3; $Z = 4$; R1 = 0.036; and wR2 = 0.072 (all data). The structure of $[Ba_3(O_3PCH_2NH_2CH_2PO_3)_2(H_2O)_4]\cdot 3H_2O$ is built up from BaO_8 and BaO_{10} polyhedra forming BaO chains and layers, respectively. These are connected to a three-dimensional metal–oxygen–metal framework with the iminobis(methylphosphonic acid) formally coating the inner walls of the pores. The one-dimensional pores (3.6×4 Å) are filled with H_2O molecules that can be thermally removed. Thermogravimetric investigations and temperature-dependent X-ray powder diffraction demonstrate the stability of the crystal structure up to 240 °C. The uptake of *N*,*N*-dimethylformamide and H_2O by dehydrated samples is demonstrated. Furthermore, IR, Raman, and ^{31}P magic-angle-spinning NMR data are also presented.

Introduction

Metal phosphonates belonging to the class of inorganic−organic hybrid materials have attracted widespread interest as a result of their ability to form interesting structures with potential applications as sorbents, ion exchangers, catalysts, or charge-storage materials.[1] These materials may be conveniently divided into two categories: coordination polymers with an extended array composed of metal−oxygen clusters bridged by polyfunctional organic molecules and hybrid metal oxides that contain infinite metal−oxygen−metal (M−O−M) arrays as part of their structure.[2] In contrast to the M(IV) phosphonates where mostly layered or pillared materials are observed, M(II) and M(III) monophosphonates show a larger variety of crystal structures that range from molecular to one-dimensional, two-dimensional, and three-dimensional (3D) structures. Only a few of these materials exhibiting a 3D structure show an open-framework structure that would be desirable for their application as molecular sieves, ion exchange materials, or catalytic materials. The introduction of porosity into the metal(II) and metal(III) phosphonates has been a major effort in recent years. The following different strategies have been investigated: (1) the use of phosphate and phosphite ions in the synthesis of pillared metal phosphonate compounds, (2) the use of metal ions that do not adopt an octahedral environment, and (3) the use of polyfunctionalized phosphonic acids. Although these strategies lead, in some cases, to open-framework structures, no general method has been found up to now.[3]

* To whom correspondence should be addressed. Tel.: +49-431-880-1675. Fax: +49-431-880-1775. E-mail: stock@ac.uni-kiel.de.
[†] Christian-Albrechts-University.
[‡] Ludwig-Maximilians-Universität München.

(1) (a) Cheetham, A. K.; Férey, G.; Loiseau, T. *Angew. Chem., Int. Ed.* **1999**, *38*, 3268.
(2) Forster, P. M.; Cheetham, A. K. C. *Top. Catal.* **2003**, *24*, 79.
(3) Clearfield, A. Metal Phosphonate Chemistry. In *Progress in Inorganic Chemistry*; Karlin, K. D., Ed.; John Wiley: New York, 1998; Vol. 47, pp 371−510.

10.1021/ic050935m CCC: $30.25
Published on Web 10/25/2005

Despite the large interest in metal phosphonates over the last two decades, only a small number of barium phosphonates have been reported up to now. Three barium hydrogenphosphonates, $Ba(HO_3PC_6H_5)_2$,[4] $Ba(HO_3PC_6H_4PO_3H)$,[5] and $Ba(HO_3PC_6H_4C_6H_4PO_3H)$,[5] having layers composed of eight-coordinate Ba^{2+} ions and phosphonate groups, are formed. All three compounds are structurally related and exhibit the same Ba−O−P topology. Whereas in the monophosphonate a layered structure is formed, the two bisphosphonates crystallize in a pillared structure. All three compounds exhibit no porosity. The other structurally characterized Ba phosphonate, a coordination polymer of Ba^{2+} ions, is the dichloromethylene bisphosphonic acid *P*,*P*′-diethylester, $Cl_2C(PO_3HEt)_2$, which has the composition $[(H_2O)_2Ba\{Cl_2C(PO_3Et)_2\}_2Ba(H_2O)_2]_n$[6] and also contains eight coordinated Ba^{2+} ions. As can be anticipated from the formula, two adjacent barium ions are joined by two $Cl_2C(PO_3Et)_2^{2-}$ ligands. These dimeric units are further bridged through oxygen atoms of the $Cl_2C(PO_3Et)_2^{2-}$ and the aqua ligands, thus, forming the polymeric chains.

Alkyliminobis(methylphosphonic acids), $RN(CH_2-PO_3H_2)_2$, for example, with R = $-CH_3$, $-CH_2CH_3$, and derivatives, such as $HOOC-CH_2-N(CH_2PO_3H_2)_2$, $H_2O_3P-CH_2-N(CH_2PO_3H_2)_2$, or $HOOC-CH_2-C_6H_4-CH_2-N(CH_2PO_3H_2)_2$, have been of interest as a result of their complex coordination behavior and their ability to possibly adopt various kinds of coordination modes and hydrogen bonding.[7] Very few crystallographic studies have been published on the use of the "parent" iminobis(methylphosphonic acid), $HN(CH_2-PO_3H_2)_2$, in the synthesis of metal phosphonates, but the pH-dependent complexation behavior in aqueous solutions toward Zn^{2+}, Mg^{2+}, and Ca^{2+} has been described.[8] Thus, only compounds with Cu^{2+},[9,10] Pb^{2+},[11] and Co^{2+} [12,13] ions have been obtained up to now. In the crystal structure of $Pb(HO_3PCH_2NHCH_2PO_3H)$, the Pb^{2+} and $(HO_3PCH_2NHCH_2PO_3H)^{2-}$ ions form a 3D framework containing PbO_5 polyhedra. Large rings were observed that collapse into the void as a result ofthe high flexibility of the organic unit. The investigation of the coordination behavior of $HN(CH_2PO_3H_2)_2$ toward Co^{2+} ions was started as a result of the presence of phosphonate moieties in biological fluids and, therefore, is of interest for the ion transport in biological systems.

We are interested in the synthesis of polyphosphonic and phosphonocarboxylic acids and in their use in the synthesis of new metal phosphonates, with the goal of obtaining 3D channel structures. Whereas the systematic investigation employing the diphosphonic acid $H_2O_3PCH_2C_6H_4CH_2PO_3H_2$ and its tetraethyl ester has led to a number of new pillared structures[14,15] and one layered structure,[16] the focus of our recent work has been the use of phosphonic acids containing iminobis(methylphosphonic acid) units, $(H_2O_3PCH_2)_2N$. Thus, the reaction of $(H_2O_3PCH_2)_2N-(CH_2)_4-N(CH_2PO_3H)_2$,[17,18] $(H_2O_3PCH_2)_2N-CH_2C_6H_4CH_2-N(CH_2PO_3H)_2$,[19] and $(H_2O_3PCH_2)_2N-CH_2C_6H_4COOH$[20] with different metal ions has led to a number of new compounds, some containing 3D framework structures and one showing reversible dehydration/hydration properties.[19]

In this paper we describe the synthesis and detailed characterization of the barium diphosphonate $[Ba_3(O_3PCH_2NH_2CH_2PO_3)_2(H_2O)_4]\cdot 3H_2O$ that was first obtained as a side product as a result of the in situ decomposition of $HOOC-C_6H_4-CH_2N(CH_2PO_3H_2)_2$. The synthesis, using the decomposition product $HN(CH_2PO_3H_2)_2$ as a starting material, was optimized to allow a detailed characterization of the title compound.

Experimental Section

For this investigation different synthesis setups were used, which are shown in Figure 1. The synthesis method commonly employed in hydrothermal reactions is the dissolution or suspension of all the starting materials in one reactor (Figure 1B). In addition, two diffusion-controlled setups were used. The setup was constructed by placing a small Teflon reactor (7-mm diameter and 13 mm high, $V_{max} = 500\ \mu L$) in a larger Teflon reactor (23 mL, Parr instruments). In setup 1A, the barium salt was placed in the smaller Teflon reactor, which was placed in the larger one containing the phosphonic acid. The starting materials were carefully covered with the solvent, and the level was adjusted just above the rim of the smaller reactor. In setup 1C, the phosphonic acid was placed in the smaller Teflon reactor, which was placed in the larger one containing the barium salt. The starting materials were carefully covered with the solvent, and the level was adjusted just above the rim of the smaller reactor.

Synthesis. $(H_2O_3PCH_2)_2NCH_2C_6H_4COOH$ was synthesized by a Mannich-type reaction, according to the literature, starting from *p*-methylaminebenzoic acid. $(H_2O_3PCH_2)_2NH$ (Aldrich) and $Ba(OH)_2\cdot 8H_2O$ (Merck) were used as obtained.

Single crystals of $[Ba_3(O_3PCH_2NH_2CH_2PO_3)_2(H_2O)_4]\cdot 3H_2O$ were obtained with $(H_2O_3PCH_2)_2NCH_2C_6H_4COOH$ as the starting material. The reactor system 1A was used, and 59.9 mg (0.19 mmol) of $Ba(OH)_2\cdot 8H_2O$ (Merck) was placed in the small Teflon reactor. An aliquot of 64.4 mg (0.19 mmol) of $(H_2O_3PCH_2)_2NCH_2C_6H_4COOH$ together with 75 μL of 2.5 M NaOH was placed in the 23-mL polytetrafluoroethylene (PTFE) liner. Both were covered

(4) Poojary, D. M.; Zhang, B.; Cabeza, A.; Aranda, M. A. G.; Bruque, S.; Clearfield, A. *J. Mater. Chem.* **1996**, *6*, 639.
(5) Poojary, D. M.; Zhang, B.; Clearfield, A. *Anales Quim., Int. Ed.* **1998**, *94*, 401.
(6) Kontturi, M.; Vuokila-Laine, E.; Peraniemi, S.; Pakkanen, T. T.; Vepsalainen, J. J.; Ahlgren, M. *J. Chem. Soc., Dalton Trans.* **2002**, 1969.
(7) Sharma, C. V. K.; Clearfield, A. *J. Am. Chem. Soc.* **2000**, *122*, 4394.
(8) Matczak-Jon, E.; Kurzak, B.; Kamecka, A.; Sawka-Dobrowolska, W.; Kafarski, P. *J. Chem. Soc., Dalton Trans.* **1999**, 3627.
(9) Cabeza, A.; Bruque, S.; Guagliardi, A.; Aranda, M. A. G. *J. Solid State Chem.* **2001**, *160*, 278.
(10) Kong, D.; Li, Y.; Ross, J., Jr.; Clearfield, A. *Chem. Commun.* **2003**, 1720.
(11) Stock, N. *Solid State Sci.* **2002**, *4*, 1089.
(12) Jankovics, H.; Daskalakis, M.; Raptopoulou, C. P.; Terzis, A.; Tangoulis, V.; Giapintzakis, J.; Kiss, T.; Salifoglou, A. *Inorg. Chem.* **2002**, *41*, 3366.
(13) Turner, A.; Jaffres, P.-A.; MacLean, E. J.; Villemin, D.; McKee, V.; Hix, G. B. *J. Chem. Soc., Dalton Trans.* **2003**, 1314.
(14) Stock, N.; Bein, T. *J. Solid State Chem.* **2002**, *167*, 330.
(15) Irran, E.; Stock, N.; Bein, T. *J. Solid State Chem.* **2003**, *173*, 293.
(16) Stock, N.; Guillou, N.; Bein, T.; Férey, G. *Solid State Sci.* **2003**, *5*, 629.
(17) Stock, N.; Bein, T. *Angew. Chem., Int. Ed.* **2004**, *43*, 749.
(18) Stock, N.; Rauscher, M.; Bein, T. *J. Solid State Chem.* **2004**, *177*, 642.
(19) Stock, N.; Stoll, A.; Bein, T. *Microporous Mesoporous Mater.* **2004**, *69*, 65.
(20) Bauer, S.; Stock, N.; Bein, T. *Inorg. Chem.* **2005**, *44*, 5882.

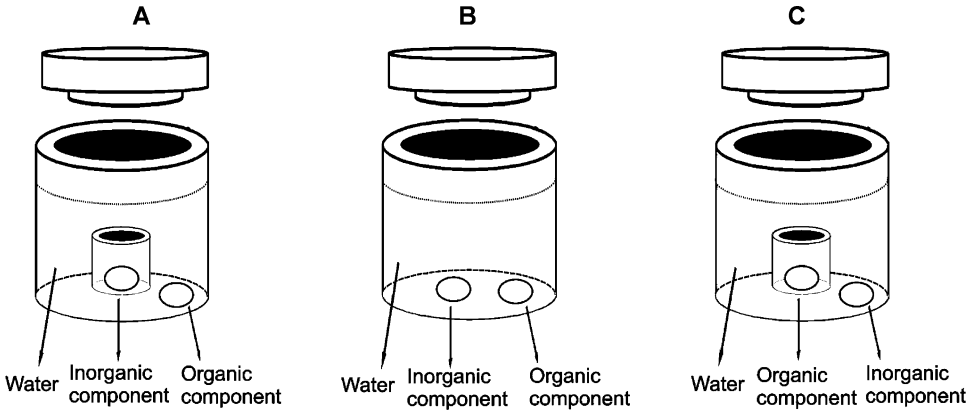

Figure 1. Three reaction systems were employed in this study: A, diffusion-controlled setup with an inner reactor with Ba^{2+} salt and the phosphonic acid in the larger Teflon reactor; B, common setup with the solution or suspension in one Teflon reactor; C, diffusion-controlled setup with an inner reactor with phosphonic acid and the Ba^{2+} salt in the larger Teflon reactor.

with H_2O and sealed in a stainless steel autoclave (Parr, U.S.A.). The reaction was carried out at 175 °C for 24 h under autogenous pressure. The resulting product, containing large single crystals of the title compound and an X-ray amorphous powder, was filtered and washed thoroughly with deionized water. The final pH was ~7. Several single crystals were tested by single-crystal X-ray diffraction (XRD). [The scanning electron microscopy (SEM) micrograph of a well-shaped single crystal is shown in Supporting Information.]

Single-phase microcrystalline $[Ba_3(O_3PCH_2NH_2CH_2PO_3)_2(H_2O)_4]\cdot 3H_2O$ was obtained by using $(H_2O_3PCH_2)_2NH$ as the starting material. The reactor system 1C was used, and 38.9 mg (0.19 mmol) of $(H_2O_3PCH_2)_2NH$ was placed in the small Teflon reactor. An aliquot of 64.4 mg (0.19 mmol) of $Ba(OH)_2\cdot 8H_2O$ together with 5 μL of 2 M HCl was placed in the 23-mL PTFE liner. Both were covered with H_2O and sealed in a stainless steel autoclave (Parr, U.S.A.). The reaction was carried out at 175 °C for 24 h under autogenous pressure. The final pH was ~5. The resulting microcrystalline product was filtered and washed thoroughly with deionized water. The X-ray powder diagram compares well with the simulated X-ray pattern calculated from the single-crystal data (see Supporting Information).

For solvent exchange studies, the as-synthesized material was partially dehydrated at 125 °C and immersed in the solvent of choice [*N*,*N*-dimethylformamide (DMF), H_2O, or methanol]. The stability of the dehydrated sample was confirmed by XRD measurements. After 24 h, the product was filtered and washed with acetone three times. After drying in air, IR spectra were recorded. Rehydrated samples were checked by thermogravimetric analysis (TGA) measurements.

Characterization. IR spectra were recorded on a Bruker IFS 66v/S Fourier transform infrared (FTIR) spectrometer in the spectral range of 4000−400 cm^{-1} using the KBr disk method. The Raman spectra were recorded using a FRA 106/S Raman module attached to a Bruker EQUINOX 55 FTIR spectrometer. An excitation wavelength of 1064 nm was used.

TGA was performed using a Setaram TG-DTA92 apparatus (heating rate: 5 °C/min) in a helium atmosphere performing simultaneously TGA and differential thermal analysis/differential scanning calorimetry measurements. Several steps in the TGA curve are observed (Figure 2). The weight loss already starts at room temperature (RT) in the gas atmosphere. Therefore, the first weight loss up to 200 °C (5.2 molecules of water per formula unit) is smaller than expected and can be attributed to the loss of water molecules. Weight losses between 300 and 400 °C and between

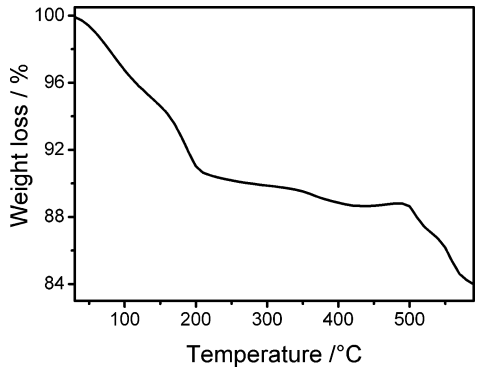

Figure 2. Results of the TGA investigation of $[Ba_3(O_3PCH_2NH_2CH_2PO_3)_2(H_2O)_4]\cdot 3H_2O$.

475 and 600 °C can be associated with the decomposition of the organic moiety. This is supported by the temperature-dependent X-ray powder diffraction experiment.

The ^{31}P magic-angle-spinning (MAS) NMR spectra were recorded on a DSX Avance FT spectrometer (Bruker) using a 2.5-mm ZrO_2 rotor. The collection was performed using a four-step phase cycled single-pulse acquisition with a repetition delay of 80 s. The spinning speed was varied between 10 and 15 kHz. During the acquisition time, two-pulse phase modulation broad-band proton decoupling was used with a 15° phase alternation.[21] The chemical shifts are referenced to the ^{31}P resonance in 85% H_3PO_4. The ^{31}P spectrum shows two signals at 9.9 and 7.6 ppm and, thus, points to the presence of two independent P atoms in similar coordination environments.

X-ray powder diffraction was carried out using a STOE STADI P transmission powder diffractometer. The samples were enclosed in capillaries (inner diameter of 0.3 mm) and measured using Mo Kα radiation. For the temperature-dependent XRD experiment, powder patterns were recorded every 15 °C between RT and 600 °C using Mo Kα radiation (Figure 3). Up to 240 °C, reflections that correspond to the title compound and its dehydration products can be observed. Between 240 and 430 °C, an X-ray amorphous product is formed. At higher temperatures, reflections are observed in the XRD pattern that do not correspond to any published Ba−phosphate phase.

SEM micrographs and energy dispersive X-ray (EDX) analyses were realized on a JEOL JSM6500F field-emission electron

(21) Bennett, A. E.; Rienstra, C. M.; Auger, M.; Lakshimi, K. V.; Griffin, R. G. *J. Chem. Phys.* **1995**, *103*, 6951.

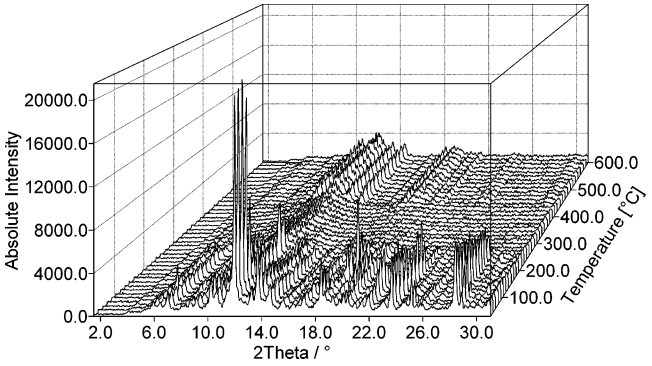

Figure 3. Temperature-dependent XRD of $[Ba_3(O_3PCH_2NH_2CH_2PO_3)_2(H_2O)_4]\cdot 3H_2O$.

microscope equipped with an Oxford instruments EDX detector. The molar ratio Ba/P of 1:2 was observed.

All these analyses are in agreement with the results deduced from the structure determination of $[Ba_3(O_3PCH_2NH_2CH_2PO_3)_2(H_2O)_4]\cdot 3H_2O$.

Crystal Structure Determination. The single-crystal structure determination by XRD was performed on a STOE IPDS diffractometer with Mo Kα radiation operating at 55 kV and 50 mA. A suitable single crystal was carefully selected under a polarizing microscope. The data reduction and absorption correction was carried out using Xred.[22] The single-crystal structure was solved by direct methods and refined using the programs SHELXS and SHELXL.[23] H atoms connected to C atoms were placed onto calculated positions, and the ones bonded to the N atom and the water molecules could not be located from the difference Fourier maps. The H atoms were refined using a riding model and by fixing the temperature factor to be 1.2 times the value of the atom to which they were bonded. Details of the structure determination are given in Table 1. Atomic coordinates, bond distances, and angles are presented in Table 2.

Cambridge crystallographic data center (CCDC) 235428 contains the supplementary crystallographic data for this paper. These data can be obtained free of charge via the Internet at www.ccdc.cam.ac.uk/conts/retrieving.html (or from the CCDC, 12 Union Road, Cambridge CB2 1EZ, U.K.; fax, +44 1223 336033; e-mail, deposit@ccdc.cam.ac.uk).

Results and Discussion

Synthesis. The synthesis of $[Ba_3(O_3PCH_2NH_2CH_2PO_3)_2(H_2O)_4]\cdot 3H_2O$ was investigated using different setups, according to Figure 1. Large single crystals of **1** have only been obtained by starting from $(H_2O_3PCH_2)_2NCH_2C_6H_4COOH$. In situ decomposition, according to Figure 4, leads to the formation of iminobis(methylphosphonic acid), which reacts with the Ba^{2+} ions to form the title compound. This leads only to small amounts of $HN(CH_2PO_3H_2)_2$ in the synthesis mixtures and, thus, a slow formation of **1**. This slow release of $HN(CH_2PO_3H_2)_2$ seems to be mandatory, because up to now, starting directly from $HN(CH_2PO_3H_2)_2$, only diffusion-controlled reactions have led to the formation of microcrystalline **1**. The title compound is observed in reaction mixtures with a final pH value from 4 to 7 in the temperature range of 155−175 °C. Above 175 °C, only X-ray amorphous materials or clear solutions were obtained. At pH < 4, no solid reaction products could be isolated. Working in reaction system B led only to X-ray amorphous compounds, while reaction systems A and C were successfully used in the synthesis of **1**.

Table 1. Crystallographic Data for $[Ba_3(O_3PCH_2NH_2CH_2PO_3)_2(H_2O)_4]\cdot 3H_2O$

space group	*C*2/*c*
crystal system	monoclinic
a (pm)	2328.7(2)
b (pm)	1359.95(7)
c (pm)	718.62(6)
β (deg)	98.732(10)
V (10^6 pm^3)	2249.5(3)
Z	4
formula mass	942.13
ρ (g/cm^3)	2.800
F(000)	1800
crystal size (mm^3)	0.20 × 0.10 × 0.03
μ (mm^{-1})	5.568
absorption correction	numerical
T_{min}/T_{max}	0.4577/0.8471
2θ range (deg)	3.0−27.93
range in *h*, *k*, and *l*	$-30 \le h \le 30$, $-17 \le k \le 16$, $l \le 8$
total data collected	2677
unique/obs. data [$I > 2\sigma(I)$]	2677/2298
R(int)	0.0527
R1, wR2 [$I > 2\sigma(I)$]	0.0293, 0.0696
R1, wR2 (alle Daten)	0.0364, 0.0715
goodness of fit	1.051
number of parameters	162
$\Delta e_{min}/\Delta e_{max}$ (e Å^{-3})	−1.765/1.652

Table 2. Selected Bond Distances (Å) and Angles (deg) for $[Ba_3(O_3PCH_2NH_2CH_2PO_3)_2(H_2O)_4]\cdot 3H_2O$

bond distances (Å)			
Ba1−O5 (2×)	2.630(3)	Ba2−O1	2.728(3)/2.844(3)
Ba1−O5 (2×)	2.729(3)	Ba2−O2	2.844(3)/2.969(3)
Ba1−O6 (2×)	2.947(3)	Ba2−O3	2.983(3)/2.885(3)
Ba1−O9 (2×)	2.960(9)	Ba2−O4	2.690(3)/2.812(3)
		Ba2−O6	3.069(3)
		Ba2−O7	2.979(4)
P1−O1	1.517(3)	P2−O4	1.507(3)
P1−O2	1.524(3)	P2−O5	1.519(3)
P1−O3	1.528(3)	P2−O6	1.530(3)
P1−C1	1.821(5)	P2−C2	1.824(4)
N1−C1	1.490(6)	N1−C2	1.485(5)
bond angles (deg)			
O1−P1−O2	113.48(18)	O4−P2−O5	115.09(19)
O1−P1−O3	111.59(18)	O4−P2−O6	112.08(18)
O2−P1−O3	111.74(19)	O5−P2−O6	110.31(18)
O1−P1−C1	107.2(2)	O4−P2−C2	108.7(2)
O2−P1−C1	106.5(2)	O5−P2−C2	101.96(19)
O3−P1−C1	105.9(2)	O6−P2−C2	108.0(2)
C2−N1−C1	113.0(3)	N1−C1−P1	112.7(3)
N1−C2−P2	115.7(3)		

Structure Description. The structure of $[Ba_3(O_3PCH_2NH_2CH_2PO_3)_2(H_2O)_4]\cdot 3H_2O$ is built up from 17 crystallographically independent non-hydrogen atoms and is comprised of two C atoms, one N atom, two PO_3 groups, two Ba atoms, two aqua ligands (O7, O9), and two noncoordination water molecules (O8, O10; Figure 5). Figure 6 shows the two independent Ba^{2+} ions forming $Ba(1)O_8$ and $Ba(2)O_{10}$ polyhedra as well as the coordination behavior of the $[O_3PCH_2NH_2CH_2PO_3]^{3-}$ ions. Ba(1) ions are connected to zigzag chains of edge-sharing polyhedra, and the Ba(2) ions form a 3D net of corner- and face-sharing polyhedra. The

(22) *XRED*, version 1.09; data reduction and absorption correction program for Windows; Stoe & Cie GmbH: Darmstadt, Germany, 1997.

(23) Sheldrick, G. M. *SHELXS-97*; Program for the solution of crystal structures; Universität Göttingen: Göttingen, Germany, 1997. Sheldrick, G. M. *SHELXL-97*; Program for the refinement of crystal structures; Universität Göttingen: Göttingen, Germany, 1997.

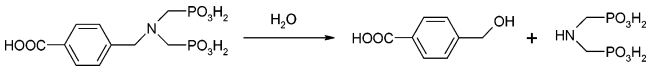

Figure 4. In situ decomposition of the phosphonocarboxylic acid and formation of the iminobis(methylphosphonic acid).

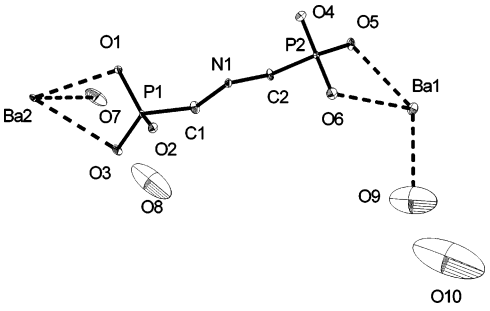

Figure 5. Asymmetric unit of $[Ba_3(O_3PCH_2NH_2CH_2PO_3)_2(H_2O)_4]\cdot 3H_2O$. Thermal ellipsoids are shown at the 95% probability level, except the water molecules, which are shown with 75% probability.

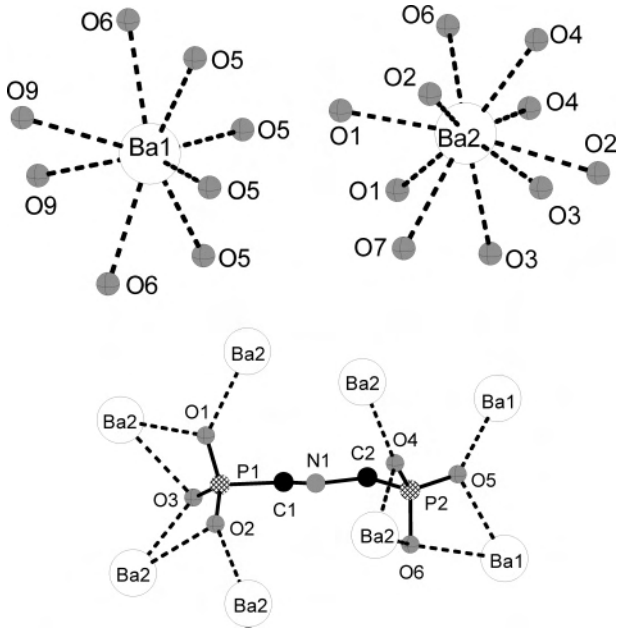

Figure 6. View of the coordination polyhedra $Ba(1)O_8$ and $Ba(2)O_{10}$ of the two crystallographically independent Ba^{2+} ions (top) and the coordination behavior of $[O_3PCH_2NH_2CH_2PO_3]^{3-}$ (bottom) in $[Ba_3(O_3PCH_2NH_2CH_2PO_3)_2(H_2O)_4]\cdot 3H_2O$.

crystal structure can be thought to be built up from these zigzag chains that connect the layers to a 3D Ba−O framework (Figures 7 and 8). Thus, this compound is a rare example of a hybrid metal oxide exhibiting a 3D M−O−M framework.[2] The phosphonate units can be thought of as lining the inner wall of the BaO network and, thus, further stabilizing the structure. Seven water molecules per formula unit are located (Figure 9) in the channels, with O7 and O9 coordinatively bonded to Ba(1) and Ba(2), respectively. Therefore, the formula is written as $[Ba_3(O_3PCH_2NH_2CH_2PO_3)_2(H_2O)_4]\cdot 3H_2O$. The water molecules can be removed by thermal treatment, as shown by TGA (Figure 2) and by temperature-dependent X-ray powder-diffraction experiments (Figure 3). Treating the dehydrated compound with DMF or water leads to the incorporation of the solvent molecules. This was confirmed by IR spectroscopy (Figure 10) through the presence of a well-defined band at 1657 cm^{-1}, which can be attributed to the C=O vibration of DMF.

The coordination behavior of the tetraphosphonic acid is shown in Figure 6. All oxygen atoms of the diphosphonic unit act as bridging (μ_2-oxygen) units; thus, each oxygen is bridging two Ba^{2+} ions. Thus, a 222 coordination mode for the phosphonate groups is observed.

The interatomic distances are well-defined. The barium−oxygen distances, Ba(1)−O = 2.630(3)−2.960(9) (8×) and Ba(2)−O = 2.690(3)−3.069(3) (10×), correspond well with the sum of the ionic radii [1.21 + 1.56 (1.66) = 2.77 (2.87) Å for 8- and 10-coordinated Ba^{2+} ions, respectively][24] and the values observed in other phosphonates.[4,5,6] For charge compensation, one proton has to be present but could not be located in the structure determination. Theoretically, the proton can be located either in the framework or in the channels as an H_3O^+ ion. The protonation of one of the phosphonate groups seems unreasonable because the coordination mode of both of the O_3P groups is the same (222) and the bonding distances of P(1)−O [1.517(3)−1.528(3)] and P(2)−O [1.507(3) − 1.530(3)] are very similar. This is also supported by the results of the ^{31}P MAS NMR investigation, where similar chemical shifts at 7.55 and 9.93 ppm are observed (Supplementary Information). The vibrational studies also give no hint of the presence of HO_3P groups, because no broad absorption bands in the region between 2200 and 2800 cm^{-1} are observed. As a result of the presence of the amine functionality, the protonation of the framework should take place. Therefore, the protonation of the amino group seems most reasonable and is also in accordance with the expected pK_a values of phosphonic acids and amines. In addition, this is also supported by the other structurally characterized compounds, such as $Cu_3[(O_3PCH_2)_2NH_2]_2$[9] or $Ca[(HO_3PCH_2)_2N(H)-CH_2C_6H_4CH_2-N(H)(CH_2PO_3H)_2]\cdot 2H_2O$.

Thermal Behavior. The thermal stability of $[Ba_3(O_3PCH_2NH_2CH_2PO_3)_2(H_2O)_4]\cdot 3H_2O$ has been studied using temperature-dependent X-ray powder diffraction measurements (Figure 3). The data demonstrate that **1** is stable up to 240 °C. The departure of water does not lead to large structural changes but only to changes in scattering intensities. Therefore, the observed reflections correspond to the title compound and its dehydration products. Between 240 and 430 °C, an X-ray amorphous product is formed. At higher temperatures, reflections are observed in the XRD pattern that do not correspond to any published Ba−phosphate phase. These values are in agreement with the TGA results (Figure 2).

IR and Raman Spectroscopic Study. The IR and Raman spectra of $[Ba_3(O_3PCH_2NH_2CH_2PO_3)_2(H_2O)_4]\cdot 3H_2O$ are shown in Figure 10 and in Supporting Information. The spectra show similarities to the ones published for $Al[(HO_3PCH_2)_3N]\cdot H_2O$ and $Cu_3[(O_3PCH_2)_3NH_2]_2$.[9] The broad adsorption bands at 3400 and 3190 cm^{-1} in the IR spectrum clearly show the

(24) (a) Shannon, R. D.; Prewitt, C. T. *Acta Crystallogr., Sect. B: Struct. Crystallogr. Cryst. Chem.* **1969**, *25*, 925. (b) Shannon, R. D.; Prewitt, C. T. *Acta Crystallogr., Sect. B: Struct. Crystallogr. Cryst. Chem.* **1970**, *26*, 1046.

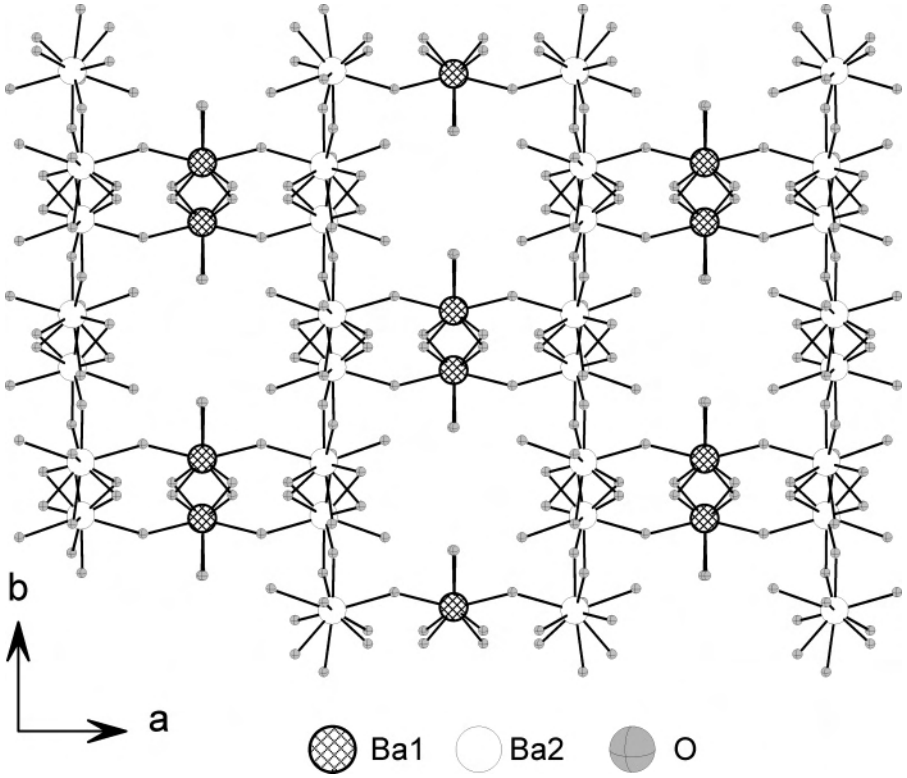

Figure 7. Connection of BaO polyhedra to strands and layers and the interconnection to a 3D framework. View along the *c* axis.

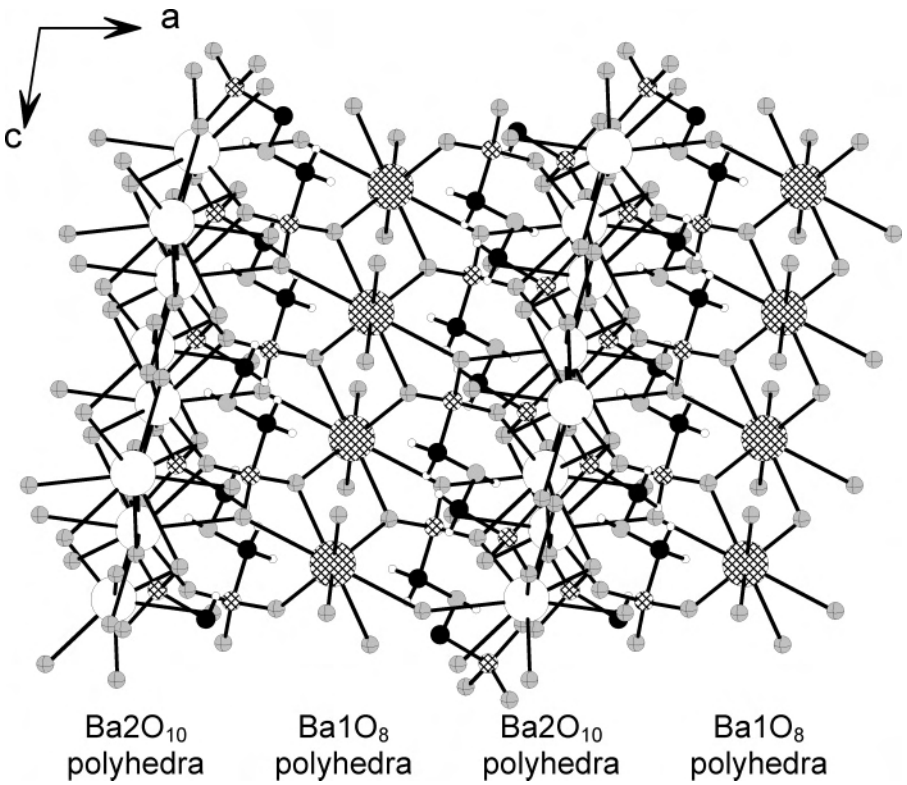

Figure 8. Structure of $[Ba_3(O_3PCH_2NH_2CH_2PO_3)_2(H_2O)_4]\cdot 3H_2O$ (view along the *b* axis). Gray-striped polyhedra represent $Ba(1)O_8$ and $Ba(2)O_{10}$, and black, gray, gray-hatched, and small white-hatched atoms represent C, N, O, and P, respectively.

presence of water molecules. The position and the width suggest that it is loosely bonded and interacting through hydrogen bonds. Whereas the C−H stretching vibrations yield only small signals in the IR spectrum, they are well-resolved and show high intensities in the Raman spectrum. They are observed at 2834/80 and 2986/44 cm^{-1} for the ν_s and ν_{as}, respectively. The sharp vibrational bands expected for the NH_2- groups at around 3030, 3000, and 1560 cm^{-1} are probably not observed as a result of the intensive water bands.[9] The intense band at 1440 cm^{-1} is typical of the CH_2

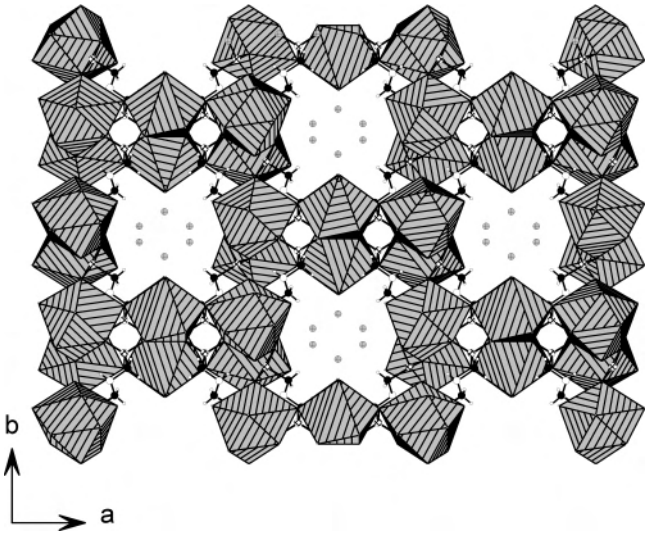

Figure 9. Structure of $[Ba_3(O_3PCH_2NH_2CH_2PO_3)_2(H_2O)_4]\cdot 3H_2O$ (view along the *c* axis). Gray-striped polyhedra represent $Ba(1)O_8$ and $Ba(2)O_{10}$, and black, gray, gray-hatched, and white-hatched atoms represent C, N, O, and P, respectively.

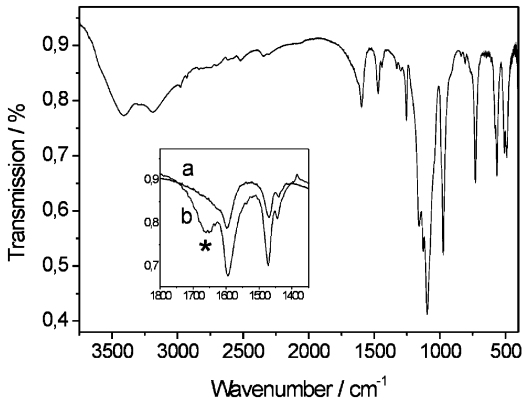

Figure 10. IR spectra of $[Ba_3(O_3PCH_2NH_2CH_2PO_3)_2(H_2O)_4]\cdot 3H_2O$ (a) and of the partially dehydrated DMF-treated title compound (b). The asterisk denotes the vibration band that can be attributed to the C═O vibration of DMF.

deformation vibration, and the band at 1250 cm^{-1} can be assigned to the P−C stretching vibration of the phosphonates. The broad bands in the IR spectrum between 1096 and 1157 cm^{-1}, as well as the sharp band at 974 cm^{-1}, are due to PO_3 and C−N stretching vibrations. According to its large intensity in the Raman spectrum, the last band is expected to be due to the ν_s of PO_3. The assignment of the remaining band is ambiguous because this complex solid has many vibrations in this region, but the similarities to the IR spectrum of $Cu_3[(O_3PCH_2)_3NH_2]_2$ are obvious.[9]

Conclusion

The in situ decomposition of $(H_2O_3PCH_2)_2NCH_2C_6H_4$-COOH resulted in single crystals of the new microporous open-framework compound $[Ba_3(O_3PCH_2NH_2CH_2PO_3)_2$-$(H_2O)_4]\cdot 3H_2O$ with a 3D M−O−M framework. For the synthesis of the pure-phase material of the title compound, the synthesis setup as well as the pH of the reaction system plays a crucial role. In addition to the elucidation of the crystal structure, the title compound was characterized in detail, and its solvent exchange property was demonstrated. Thus, $[Ba_3(O_3PCH_2NH_2CH_2PO_3)_2(H_2O)_4]\cdot 3H_2O$ is an example for microporous inorganic−organic hybrid materials built up from flexible linkers. Because the concept of reticular chemistry, as known from rigid carboxylate linkers,[25] cannot be applied to flexible building blocks for the formation of microporous hybrid materials, explorative synthesis is still necessary, because many unknown factors control the formation of the final crystal structure. Nevertheless, large cations with flexible coordination spheres in combination with small flexible bisphosphonic acids seem to lead to open structures. Future work will, therefore, be concerned with the use of large cations and polyfunctional phosphonic acids. High-throughput methods developed in our group will permit the fast and efficient evaluation of the large parameter space of these systems.[26] The results will contribute to a better understanding of the chemistry of metal phosphonates.

Acknowledgment. The authors thank E. Kiesewetter for the IR measurements, C. Mincke for the ^{31}P MAS NMR measurements, Dr. P. Mayer for the acquisition of the single-crystal data, Dr. E. Irran for the temperature-dependent XRD experiments, and BMBF for partial funding of the work.

Supporting Information Available: SEM micrograph, calculated and measured XRD powder patterns, and crystallographic information file. This material is available free of charge via the Internet at http://pubs.acs.org.

IC050935M

(25) Yaghi, O. M.; O'Keeffe, M.; Ockwig, N. W.; Chae, H. K.; Eddaoudi, M.; Kim, J. *Nature* **2003**, *423*, 705.
(26) Stock, N.; Bein, T. *Angew. Chem.* **2004**, *116*, 767. Stock, N.; Bein, T. *Angew. Chem., Int. Ed.* **2004**, *43*, 749.